

# Selective Growth of Titanium Dioxide by Low-Temperature Chemical Vapor Deposition

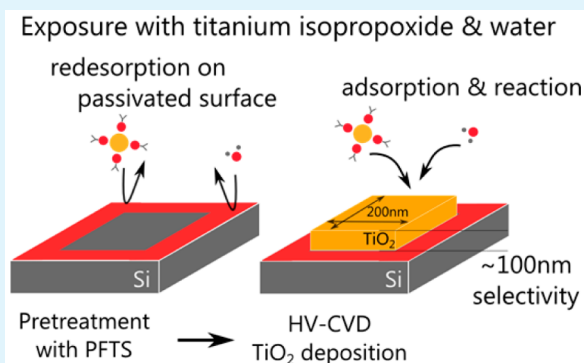
Michael Reinke,\* Yury Kuzminykh, and Patrik Hoffmann

Laboratory for Advanced Materials Processing, Empa, Swiss Federal Laboratories for Materials Science and Technology, Feuerwerkerstrasse 39, CH-3602 Thun, Switzerland

Laboratory for Photonic Materials and Characterization, Ecole Polytechnique Fédérale de Lausanne, Station 17, CH-1015 Lausanne, Switzerland

**ABSTRACT:** A key factor in engineering integrated optical devices such as electro-optic switches or waveguides is the patterning of thin films into specific geometries. In particular for functional oxides, etching processes are usually developed to a much lower extent than for silicon or silicon dioxide; therefore, selective area deposition techniques are of high interest for these materials. We report the selective area deposition of titanium dioxide using titanium isopropoxide and water in a high-vacuum chemical vapor deposition (HV-CVD) process at a substrate temperature of 225 °C. Here—contrary to conventional thermal CVD processes—only hydrolysis of the precursor on the surface drives the film growth as the thermal energy is not sufficient to thermally decompose the precursor. Local modification of the substrate surface energy by perfluoroalkylsilanization leads to a reduced surface residence time of the precursors and, consequently, to lower reaction rate and a prolonged incubation period before nucleation occurs, hence, enabling selective area growth. We discuss the dependence of the incubation time and the selectivity of the deposition process on the presence of the perfluoroalkylsilanization layer and on the precursor impinging rates—with selectivity, we refer to the difference of desired material deposition, before nucleation occurs in the undesired regions. The highest measured selectivity reached  $(99 \pm 5)$  nm, a factor of 3 superior than previously reported in an atomic layer deposition process using the same chemistry. Furthermore, resolution of the obtained patterns will be discussed and illustrated.

**KEYWORDS:** selective area growth, titanium dioxide, self-assembled monolayer, silanization, titanium isopropoxide, chemical vapor deposition, atomic layer deposition



## 1. INTRODUCTION

A key factor in engineering integrated devices such as electro-optic switches or waveguides is the patterning of thin films into specific, functional geometries. Patterning techniques can be broadly separated into in situ and ex situ techniques. While ex situ patterning is based on the selective material removal after the deposition of the films (e.g., etching), in situ techniques only locally deposit the desired material directly into the desired geometry.

Very prominent and widely used ex situ patterning techniques are physical or chemical etching processes, which are highly developed and understood for standard complementary metal–oxide–semiconductor (CMOS) compatible materials (Si, Si<sub>3</sub>N<sub>4</sub>, SiO<sub>2</sub>, etc.).<sup>1,2</sup> The constant progression and expansion of integrated circuit design functionality and the continuous miniaturization requires the development of patterning techniques also for novel materials, such as functional oxides for integrated photonic circuits.<sup>3,4</sup> Etching techniques for these materials are commonly much less developed than for established CMOS materials; hence, alternative patterning approaches need to be investigated.

Although ion beam etching can be applied to etch a great variety of materials, its practical application is often limited due to edge over etching and bottom roughening.<sup>5</sup>

Selective area chemical vapor deposition (CVD) represents an in situ approach to pattern thin films. In selective metal–organic vapor-phase epitaxy (MOVPE), the selectivity during the film growth is driven by the energetically preferable condensation of adatoms into a crystal lattice compared to the nucleation on amorphous material.<sup>6,7</sup> Here, prior to the deposition process, the substrate (Si, GaAs, ...) is masked with an amorphous template layer (native oxides), which is patterned by a wet etching step to reveal the crystalline surface substrate face, which will act as nucleation center. Furthermore, the substrate temperature must be relatively high ( $T > 750$  °C) to enable sufficient diffusion of adsorbed adatoms on the substrate surface.

Received: February 18, 2015

Accepted: April 22, 2015

Published: April 22, 2015

At CMOS compatible temperatures ( $T < 400$  °C), the surface diffusion length is not sufficiently high to achieve selectivity using this approach. Furthermore, thermal energies are usually not sufficiently high to overcome the necessary activation energy to form high-quality oxide films. Hence, for selective area CVD processes at these temperatures, precursor decomposition must be controlled in a way that enables the reaction of precursor molecules with the substrate preferably in certain regions. This can either be accomplished by local catalysis or by surface passivation prior to the deposition process.

One straightforward method to catalyze the surface reaction of precursor molecules on the substrate surface is laser-assisted CVD (LCVD)<sup>8</sup> or electron beam induced deposition (EBID),<sup>9</sup> which has been studied in great detail. Here, the deposition temperature is kept below the pyrolysis threshold of the precursor molecules, and the substrate is locally exposed to photons or electrons to induce the film growth. These techniques are usually performed in a “scanning-mode”, which leads to relatively low deposition throughput. An elegant alternative is the patterning of a layer of material by pattern projection by LCVD and completion of the growth by catalytically activated thermal CVD on the LCVD patterns. This was shown for aluminum deposition almost three decades ago.<sup>10</sup>

Another approach is to geometrically block the precursors from arriving at the surface by hard masks.<sup>11</sup> Prerequisite for this method is the use of a nonconformal deposition method, such as high-vacuum chemical vapor deposition (HV-CVD). To obtain clean selective depositions, however, it is mandatory to utilize highly reactive precursors, for example, precursors that decompose on the substrate with a high probability or precursors that exhibit a high reactive sticking coefficient. Otherwise redesorption and subsequent readsorption in geometrically shaded region leads to the formation of an undesired secondary deposit.

Generally, CVD processes are highly dependent on surface chemistry. In particular, atomic layer deposition (ALD) relies on the reaction of precursor molecules with surface terminating groups, since the deposition temperatures are purposely set below the pyrolytic decomposition threshold. In consequence, changing of the surface chemistry also modifies the reaction kinetics of a specific precursor with the substrate. Selective area ALD is based on the alteration of surface chemistry to passivate the surface, that is, restrict locally the reaction of the precursor, or activate the surface, that is, enabling locally the reaction. Mackus et. al have recently reviewed extensively the work performed in this field.<sup>12</sup> The most common approach is the passivation of the substrate surface by application of a self-assembled monolayer to reduce the surface's reactivity.<sup>13</sup> Figure 1 illustrates the general principle of this approach: by silanization the surface terminating group is altered, and hence the properties of the surface are engineered in a way that prevents the reaction of precursor with the substrate surface and thus inhibits film growth.

As the self-assembled organic monolayer is temperature-sensitive, deposition should be carried out at lowest possible deposition temperatures to keep the monolayer intact as long as possible and to ensure the highest possible selectivity. Therefore, conventional thermal CVD processes are less suitable for this approach.

Recently, we reported that deposition temperatures in CVD processes can be significantly lowered compared to conven-

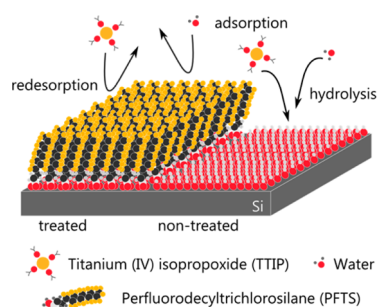


**Figure 1.** Simplified principle of selective area deposition in HV-CVD; reduced molecule interaction on the perfluorosilanized regions (using PFTS) leads to quick re-emission of the adsorbed molecules and hinders film growth compared to untreated regions.

tional thermal CVD processes. Comparable to ALD processes, a reactive partner is utilized to complete the surface reaction of the chemisorbed precursor on the substrate. This is only possible in a high-vacuum environment, where precursor transport takes place in the molecular flow regime and collisions between reactive partners in the gas phase are suppressed. Hence, the reactive partners react only on the substrate surface. Consequently, ALD chemistry (precursors) can be used in a continuous manner without need for a pulsed precursor supply. In this contribution we report on the selective area deposition of titanium dioxide using a typical ALD chemistry, namely, titanium tetraisopropoxide (TTIP) and water, in a low-temperature HV-CVD process. Titanium dioxide is an interesting material for many applications: because of its high refractive index and good transmittance in the visible and infrared spectrum, it is an appealing material for integrated optical applications. Additionally, titania films can become conductive (transparent conductive oxide) when doped with niobium.<sup>14</sup> We used perfluoroalkylsilanization to reduce locally the surface energy and render the surface oil- and water-repellent. This leads to a reduction of the residence time of TTIP and water on the substrate, decreases the hydrolysis rate of the titanium precursor, and effectively increases the incubation time of the deposition process. Patterning of the silanization layer was performed by a lift-off process using standard lithographic techniques. Subsequent low-temperature HV-CVD leads to the selective deposition of titanium dioxide.

Selective area atomic layer deposition of titania has been reported by different groups using several surface passivation methods. Different precursor combinations were used, among them titanium tetraisopropoxide,<sup>15–17</sup> titanium tetramethoxyoxide,<sup>18</sup> and titanium tetrachloride<sup>15,16</sup> in combination with water. Selective surface passivation was either realized using silanization with octadecyltrichlorosilane, perfluorooctyltriethoxysilane, or poly(methyl methacrylate). The reported selective pattern thickness varies between 2<sup>18</sup> and 30 nm.<sup>15,16</sup> Recently, high-resolution patterns have been realized utilizing octadecyltrichlorosilane as passivation layer and TTIP and water as reactants.<sup>19</sup> In this report, the self-assembled monolayer was partially removed after silanization by electron beam exposure. In this fashion sub-30 nm features could be grown by ALD; the deposited pattern thickness, however, did not exceed 2 nm.

In this manuscript we discuss the influence of the silanization process on the incubation time in dependence of precursor impinging rates and its influence on the selectivity of the deposition process. The controlled precursor impinging rates of

TTIP and water represent two additional degrees of freedom, which are available only in HV-CVD processes but not in ALD processes. Indeed we have found conditions where the obtainable selectivity supersedes reports of selective area deposition using the same chemistry in ALD. Furthermore, resolution of the obtained patterns will be discussed and illustrated.

## 2. EXPERIMENTAL METHODS

The selective area deposition of titanium dioxide by low-temperature HV-CVD is based on local modification of the substrate surface with the aim to decrease its reactivity toward nucleation. Hence, before the actual deposition process, the surface must be pretreated. This treatment leads to a prolongation of the deposition film growth incubation period in these regions and thereby to a selective growth of titanium dioxide.

In this section, we describe the local passivation of the surface by silanization before we discuss details about the low-temperature HV-CVD of titanium dioxide. Then we discuss the characterization of the obtained titania films.

**a. Local Surface Passivation.** The selective area growth process is based on the modification of surface chemistry. There, we locally decrease the substrate surface energy (rendering it hydrophobic) by a patterned silanization process based on a process described in literature,<sup>20</sup> which is illustrated in Figure 2.

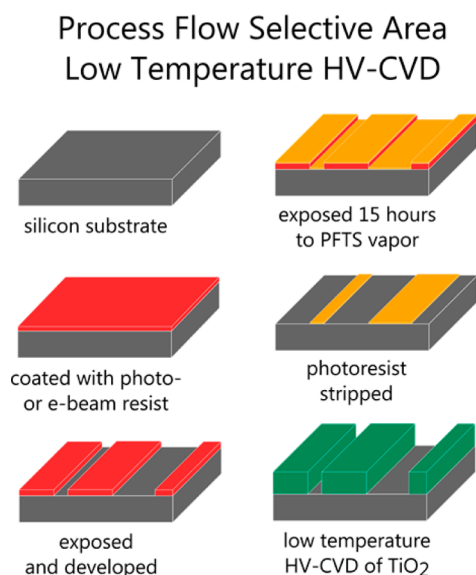


**Figure 2.** Process flow of substrate preparation and selective area deposition of titanium dioxide. Silanization is realized by exposing the substrate to PFTS in a desiccator; the substrate was previously coated with resist, which is removed after the silanization process.

The process is based on standard lithographic techniques and dependent on the desired resolution of the patterns; we used either conventional UV photolithography or e-beam lithography.

For low-resolution selective area growth processes, a 100 mm silicon substrate was spin-coated with 1.1  $\mu\text{m}$  AZ1512 photoresist, exposed ( $13 \text{ mJ cm}^{-2}$ ), and subsequently developed. The remaining photoresist acts as protection for the substrate surface as it prevents its modification during the subsequent silanization process. The regions that remain coated will render to the preferential nucleation centers in the later growth process.

We used e-beam lithography to obtain higher resolutions patterns ( $<1.5 \mu\text{m}$ ) during the selective growth. Here, we used an adapted e-beam resist (PMMA 950 K A4) and exposed it with a total dose of  $1300 \mu\text{C cm}^{-2}$  before development.

After patterned exposition of the resists and their development, the substrates were placed in a desiccator, where they were exposed for 15 h at laboratory ambient temperature to perfluorodecyltrichlorosilane vapor (PFTS, CAS 78560-44-8) for the silanization of the substrate. Afterward, the substrates were extensively rinsed in acetone and deionized water to remove the remaining resist and clean the substrate surface. Afterward we introduced the substrates into the HV-CVD reactor for the selective area growth.

**b. Low-Temperature High-Vacuum Chemical Vapor Deposition.** We deposited all thin films by low-temperature HV-CVD using titanium tetraisopropoxide (TTIP) and water as reactive species. We recently reported that these two precursors can be used simultaneously in a high-vacuum environment to grow titanium dioxide films at temperatures below the pyrolytic decomposition threshold of the titanium precursor.<sup>21</sup> Contrary to conventional CVD systems, the high-vacuum environment ensures that precursor reactions only occur on the substrate surface and that even highly reactive precursor combinations do not react already in the gas phase, which would be detrimental for the deposition process. In fact, the mean free path of TTIP and water inside the main reaction chamber exceeds its trajectory between precursor source and substrate—therefore precursor collisions are inhibited. In our experimental conditions, the pressure in the main chamber did not exceed  $1 \times 10^{-5}$  hPa during the deposition process, leading to a mean free path of  $\sim 2$  m, whereas the trajectory between precursor source and substrate is smaller than 20 cm. Hence, typical ALD precursor chemistries can be used to grow thin films in HV-CVD conditions within the so-called ALD window, that means at substrate temperatures below the pyrolytic decomposition threshold of the titanium precursor and thus at lower temperatures than in usual CVD processes. The continuous precursor substrate exposure (in contrast to ALD) enables higher growth rates for uniform films, at the cost of compromising the conformality. For the presented application, fortunately, the loss of conformality is less crucial, since processes relying on photo- or e-beam lithography for the selective surface passivation are usually nonconformal as well. As in the case of ALD processes, we found that the film is not growing directly after the precursor exposure is started, but that an incubation period precedes the nucleation. During this initial phase of the process no film is growing as reported in detail earlier.<sup>21</sup>

Working at low deposition temperature is critical for selective area deposition processes based on surface silanization, since the self-assembled monolayer becomes unstable at substrate temperatures above  $300 \text{ }^\circ\text{C}$ .<sup>22</sup> All low-temperature depositions reported here were performed at  $225 \text{ }^\circ\text{C}$  substrate temperature.

We will briefly summarize the technique and refer for more details to our recent publications.<sup>21,23</sup> Both reactive partners evaporate from separated thermalized precursor reservoirs into two separated gas pipe systems (prechambers), which lead into the high-vacuum reactor. Each prechamber possesses small orifices, which act as effusion sources for the precursors into the main reactor. If molecules diffuse through these orifices, they are directed toward the heated substrate (usually a 100 mm wafer). On the substrate, the interaction between the two precursors leads to the formation of the titanium dioxide thin film.

As described above, in the high-vacuum environment, the mean free path of the molecules is larger than the distance between effusion source and substrate; the molecules do not collide, their trajectory is a straight line, and their distribution can be described geometrically. In consequence, absolute precursor impinging rates can be relatively easily calculated analytically.<sup>11</sup>

The aim of our work was to find growth conditions yielding the highest possible selectivity for the growth of titanium dioxide on passivated and untreated surface. To do so, we performed different deposition experiments varying the TTIP impinging rate between  $3 \times 10^{14}$  and  $11 \times 10^{14} \text{ cm}^{-2} \text{ s}^{-1}$  and the water impinging rate between  $1 \times 10^{16}$  and  $6 \times 10^{16} \text{ cm}^{-2} \text{ s}^{-1}$ , always keeping the substrate temperature constant at  $225 \text{ }^\circ\text{C}$ .

**c. Characterization Methods.** The film growth was characterized in situ using a double reflectometry setup consisting of two helium neon lasers ( $\lambda = 633 \text{ nm}$ ). Reflectometry is based on the interference at the interfaces of the growing thin film. Depending on the thickness

of the deposit, the intensity of the reflected beam varies due to the interference between the reflection at the surface of the deposit and the reflection at the deposit-substrate interface. Accordingly, during the film growth, the reflectometry signal oscillates, while passing between destructive and constructive interference conditions.

We pointed two lasers at treated and untreated substrate regions and measured the intensity of their reflections by two photodiodes. In this way, we monitored the different growth behaviors on substrate regions that were treated previously by PFTS vapor (where we intend to suppress the growth) and on untreated substrate regions. Of particular interest for us was to measure how the silanization process influences the incubation time and if we can optimize the process by changing precursor fluxes.

We evaluated chemical composition and mass thickness (the mass of the thin film per unit area) *ex situ* by quantitative energy-dispersive X-ray analysis (EDX). Here, during the EDX signal fitting procedure, the interaction volume for the impinging electron beam is assumed to consist of a bilayer system of silicon and titanium dioxide—contrary to conventional evaluation algorithms that assume a homogeneous distribution of atoms within the probed volume. As described earlier,<sup>24</sup> the mass thickness of the thin films can then be evaluated by the deconvolution of the silicon signal arising from the substrate and the signal originating of the titanium and oxygen atoms. The commercial “LayerId” plugin of the Oxford Aztec software package was used for this quantitative EDX analysis.

Chemical composition and mass thickness allows us to derive the number of deposited titanium atoms per unit area. This density-independent value is a measure of the number of successful precursor decomposition processes on the substrate surface. After normalizing to the sample deposition time the growth rate in incorporated titanium atoms per unit area and unit time is determined.

We used spectroscopic ellipsometry and cross-section scanning electron microscopy to determine the film thickness of the deposits on treated and untreated substrate. Furthermore, we analyzed the films regarding their morphology and the resolution of the deposited structures by either optical or scanning electron microscopy.

### 3. RESULTS AND DISCUSSION

In this section, we present results of the silanization process and describe the optimization of growth conditions to maximize the selectivity of the deposition process. Lastly, we illustrate and discuss the obtained resolution of the structured depositions.

**a. Patterned Passivation Process.** The selective area growth is based on the alteration of surface chemistry to change the reactivity of the adsorbing precursor molecules. The above-described silanization alters the surface termination of the silicon substrate locally from hydroxyl- to trifluoromethyl groups. The different polarizabilities of the surface terminating groups lead to a reduction of van der Waals interaction between incoming precursor and the fluorinated surface compared to the untreated surface and, hence, to a decrease of the surface residence time of the TTIP molecules and water. We expect that as consequences of the reduced residence time of TTIP precursor molecules the overall reaction rate is decreased and nucleation and film growth are deferred. We quantified the efficiency of the silanization process using contact angle measurements. Because of the strong reduction of surface energy in the treated regions, the surface was rendered hydrophobic. We measured the macroscopic contact angle to be  $109^\circ \pm 2^\circ$ , which is comparable to the contact angles reported in literature for similar treatments.<sup>25</sup> The contact angle measurements were performed on a regular basis after the silanization process to ensure constant conditions. We found that relatively short exposure times (less than 4 h) to the PFTS vapor reduce the reproducibility of the surface treatment. Hence, we decided to expose all substrates longer than 12 h

(overnight) to PFTS in our desiccator setup prior to deposition.

The macroscopic contact angle gives a global impression about the quality of the silanization process. However, it does not yield information about the microscopic quality of the self-assembled monolayer. Pinholes in the functionalized coating can be detrimental to the selective area deposition process, since they can act as nucleation centers for the formation of titanium dioxide. Within this survey, we have not aimed to improve the microscopic quality of the silanization process, since we were mainly interested to study the feasibility of the process and to understand the impact of different precursor impinging rates (TTIP and water) on the selectivity of the process. Further optimization of the silanization process can improve the quality of the self-assembled monolayer. It should enhance the overall efficiency of the film growth suppression as well as further increase the incubation time difference between treated and untreated surface and hence enhance the selectivity.

**b. Selective Deposition Optimization.** After ensuring the reproducibility of the silanization process, we investigated the influence of the self-assembled monolayer on the incubation time and film growth during the low-temperature HV-CVD process. Generally, the substrate temperatures as well as the precursor impinging rates influence the duration of the incubation period. Figure 3 shows the reflectometry signal

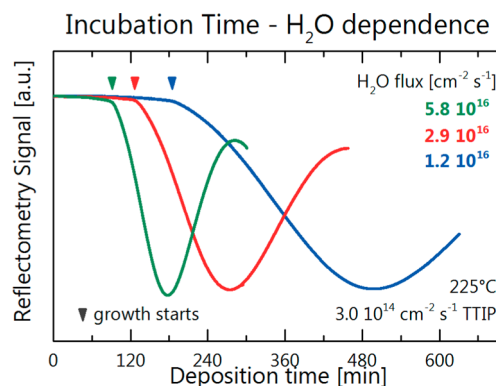


**Figure 3.** Reflectometry signal for titanium dioxide deposition on naturally oxidized silicon substrates for different water impinging rates. TTIP impinging rate is kept identical for the three depositions. The incubation time prior to film growth and the subsequent growth speed depend on the water dosage.

evolution during three deposition processes on untreated substrates at a deposition temperature of 225 °C, where we have varied the water flux but kept the TTIP impinging rate constant. The incubation period prior to film growth is visible for all three depositions. A direct comparison to ALD processes is challenging due to the very different nature of precursor exposure, which is high-flux and sequential in ALD but continuous and low-flux in HV-CVD. As indication, the incubation time during a similar ALD process usually does not exceed one or two full cycles. The total exposure dose to overcome the incubation period for both processes are however very similar, since the precursor dosage in ALD supersedes the impinging rate in HV-CVD by 2 orders of magnitude.<sup>21</sup> The end of the incubation period is characterized by the onset of the oscillation in the reflectometry signal. At the same time the oscillation period of the reflectometry signal increases with decreasing flux, which indicates that the growth rate decreases.

We studied the influence of the silanization layer on the incubation period duration with a double reflectometry setup as described in the Experimental Methods Section. The simultaneous evaluation of both surfaces, treated and untreated, ensures that we compare identical deposition conditions. Figure 4 depicts exemplary in situ reflectometry measurement results

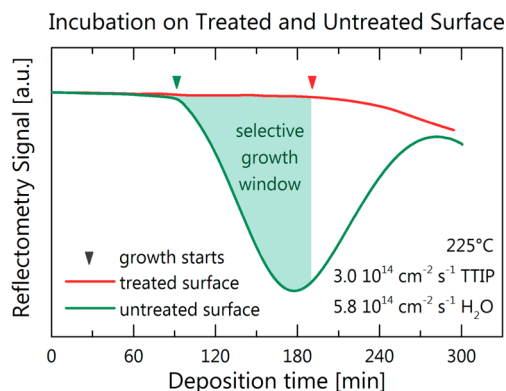


**Figure 4.** Double reflectometry setup allows us to investigate the influence of the silanization layer on the incubation period during the deposition. On the treated substrate the incubation time is significantly delayed as compared to the untreated substrate. During the time between nucleation start in untreated and treated areas titanium dioxide grows selectively.

taken during a deposition process of titanium dioxide at 225 °C substrate temperature and TTIP and water impinging rates of  $3.0 \times 10^{14} \text{ cm}^{-2} \text{ s}^{-1}$  and  $5.7 \times 10^{16} \text{ cm}^{-2} \text{ s}^{-1}$ , respectively. During the growth, one of the two laser beams (green line in Figure 4) was directed onto an untreated part of the substrate, and the other was directed onto the silanized part (red line) to measure the selectivity of the process, that is, the amount of film we can grow on the untreated surface before the nucleation on the silanization layer sets on.

Initially, we observe on both surfaces the characteristic incubation period prior to the beginning of the growth. This is

in accordance to the depositions described above. After  $\sim 85$  min, the intensity of the reflected beam pointed at the untreated surface starts to oscillate, indicating that the incubation period has ended, and a thin film starts to grow. In contrast, no film is growing on the treated substrate region as can be concluded from the constant reflectometry signal. For the next 100 min titanium dioxide is grown selectively only on the untreated substrate. After a process time of 185 min, the selective growth ends as nucleation also starts on the silanized layer as well. The time difference of the incubation times on untreated and treated regions represents the selectivity window, that is, the length of deposition that still leads to a selective area deposition.

An overview on incubation times on treated and untreated surfaces for different precursor impinging rates (water and TTIP) is shown in Figure 5a. According to results that we have reported earlier,<sup>21</sup> the incubation time decreases with increasing precursor impinging rates. We observe the same trend for the incubation time on both the treated and untreated substrate regions. The longest incubation period measured on the untreated (hydroxyl-terminated) surface is 3 h 8 min and 6 h 15 min on the treated (trifluoromethyl-terminated) surface at the lowest utilized fluxes ( $2.9 \times 10^{14} \text{ TTIP cm}^{-2} \text{ s}^{-1}$  and  $1.2 \times 10^{16} \text{ H}_2\text{O cm}^{-2} \text{ s}^{-1}$ ). The largest difference of incubation times between treated and untreated surface regions of 3 h 56 min was reached at the highest TTIP ( $11.2 \times 10^{14} \text{ cm}^{-2} \text{ s}^{-1}$ ) and the lowest water flux ( $1.2 \times 10^{16} \text{ cm}^{-2} \text{ s}^{-1}$ ). Within this time difference, the titanium dioxide film is deposited selectively only on the untreated substrate.

Simple optimization of the incubation time difference is not sufficient to gain optimal selectivity in terms of incorporated titanium atoms (or film thickness). As we stated above, different impinging rates lead also to different growth rates of the film. Hence, a short incubation time difference at a high growth rate may lead to better selectivity than a long incubation time difference at low titanium dioxide growth rates. Therefore, a comparison of incorporated titanium atoms is more suitable to determine optimal growth conditions to maximize the selectivity.

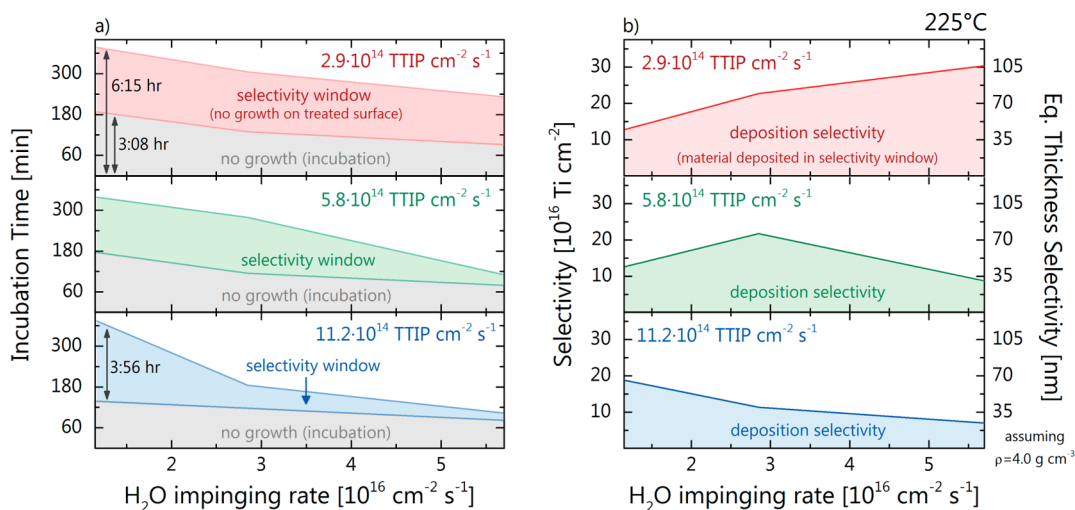


**Figure 5.** (a) Incubation times for different TTIP and H<sub>2</sub>O fluxes on treated and untreated substrates; large incubation time differences are promising for achieving highest selectivity. The maximum incubation time on untreated and treated substrate occurs at lowest TTIP and water flux, while the longest selectivity window occurs at highest TTIP and lowest water flux; (b) selectivity of the process in deposited titanium atoms per area for different precursor impinging rates; for convenience an equivalent thickness is displayed assuming a constant density of 4.0 g cm<sup>-3</sup>; the highest selectivity is not reached at the longest selectivity window but at growth conditions yielding the highest precursor deposition efficiency.

Figure 5b shows the number of incorporated titanium atoms during the incubation time difference for various TTIP and water impinging rates at a substrate temperature of 225 °C. The values were obtained by quantitative EDX analysis as described in Section 2c. Since the density of the film varies with the deposition conditions, an equivalent film thickness assuming a homogeneous density  $\rho$  of 4.0 g cm<sup>-3</sup> is given on the right scale for convenience. We calculated the equivalent film thickness  $t_{\text{eq}}$  assuming stoichiometric titanium dioxide films (atomic ratio Ti/O = 1:2) and taking the weight of a single titanium atom  $m_{\text{Ti}}$  of 47.8 u and a single oxygen atom  $m_{\text{O}}$  of 16 u using the following relation:  $t_{\text{eq}} = (n_{\text{Ti}}m_{\text{Ti}} + 2n_{\text{O}}m_{\text{O}})/\rho$ .

The deposition conditions resulting in the longest selectivity window are not the conditions where the optimal selectivity is achieved, because here the titanium incorporation rate of  $1.3 \times 10^{13}$  cm<sup>-2</sup> s<sup>-1</sup> is relatively low. The highest selectivity of  $3.0 \times 10^{17}$  cm<sup>-2</sup> was realized at low TTIP ( $2.9 \times 10^{14}$  cm<sup>-2</sup> s<sup>-1</sup>) and high water fluxes ( $5.7 \times 10^{16}$  cm<sup>-2</sup> s<sup>-1</sup>). In these conditions the incubation time difference is lower (2:21 h) than in the previous case, but the growth rate is a factor of 2.75 higher ( $3.6 \times 10^{13}$  cm<sup>-2</sup> s<sup>-1</sup>) leading to the overall higher selectivity. This absolute titanium incorporation corresponds in these conditions to a film thickness of  $(99 \pm 5)$  nm as measured by spectroscopic ellipsometry and cross-sectional scanning electron microscopy (cf. Figure 6). This supersedes the highest reported value (35 nm)<sup>15,16</sup> utilizing the same precursor chemistry in ALD conditions by a factor of 3.

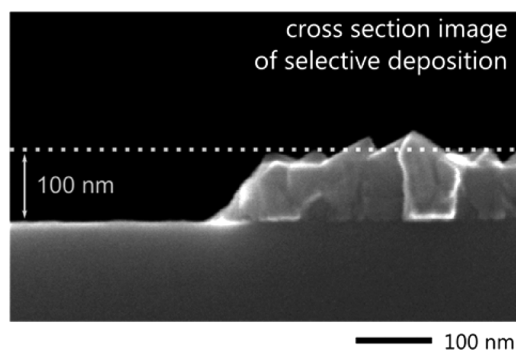


**Figure 6.** Cross-section scanning electron micrograph of the highest selectivity for the deposition of titanium dioxide on silicon of  $(99 \pm 5)$  nm by low-temperature HV-CVD.

In general, we noticed that the best selectivity is reached for conditions where the precursor deposition efficiency is high, for example, where the ratio between reacting molecules and impinging molecules is high. The deposition efficiency is the probability that an impinging titanium precursor leads to the incorporation of a titanium atom to the thin film. Earlier we reported that the highest deposition efficiency of the precursor is reached at the transition between TTIP flux limited regime (where water is dosed in excess) and water flux limited regime (where TTIP is dosed in excess) and that the highest measured deposition efficiency is 13%.<sup>21</sup> In the current case, the deposition conditions for the best selectivity lead to a deposition efficiency of 12.3%.

We believe that this connection between high precursor deposition efficiencies and high selectivity is the cause for the enhanced selectivity of HV-CVD compared to ALD as well. In ALD processes, the substrate is exposed to a high dosage of precursor molecules to ensure precursor surface saturation. In

typical conditions, the precursor impinging rate is  $\sim 1 \times 10^{18}$  cm<sup>-2</sup> s<sup>-1</sup> for a TTIP partial pressure of  $1 \times 10^{-2}$  hPa in the reactor—which is 2 orders of magnitude above the impinging rates during an HV-CVD process. The high amount of impinging TTIP molecules enhances the overall reaction probability and hence shortens the incubation duration. After the growth has started on the untreated surface, preferably all precursor molecules should contribute to the thin film formation before undesired nucleation occurs on the treated substrate. In HV-CVD, both precursor fluxes can be adapted to realize these conditions and maximize the selectivity. Conversely in ALD processes, where the precursors impinge separately from each other, and thereby prevent adjustment of the surface reaction kinetics.

**c. Process Resolution.** In this section we illustrate the deposited structures and show examples of the highest resolution patterns that we have grown so far. Figure 7 compares the photolithographic mask design that was used to locally change the surface termination by silanization to the optical micrograph of the successful low-temperature selective area deposition of titanium dioxide. Because of the higher electron density of the titanium atoms compared to the silicon atoms, the thin film appears lighter than the uncoated silicon surface. Overall, we see that our above-proposed selective area deposition process (cf. Figure 2) leads to a deposition of titanium dioxide according to the desired geometry.

We chose to deposit a variety of simple and more complex geometries; Figure 7b shows exemplary a world map representing more complex patterns. Furthermore, it shows a standard chess pattern of  $4 \times 4$   $\mu\text{m}$  squares and simple lines of either 10 or 2  $\mu\text{m}$  wide lines and spacing. All these selective area depositions were performed on substrates that we prepared by use of the sample preparation method using standard photolithography.

Higher resolution patterns are shown in Figure 8, which depicts selective area depositions on substrates that were patterned by e-beam lithography. The patterns are squares with either 800 or 200 nm side lengths. We conclude from these images that resolutions up to 200 nm are achievable with our approach.

These images also illustrate two problems, already partially mentioned above, that represent current challenges of the selective area deposition by HV-CVD. Because of the nonoptimized silanization process, the self-assembled monolayer is not perfect and most likely exhibits several pinholes, which act as nucleation centers. For this reason, even in the treated region, some titanium dioxide clusters are visible. We believe that after rigorous optimization of the silanization process, these nucleation centers can be avoided, which will lead to better results. Another possibility for the presence of small clusters within the treated region is the condensation reaction of impinging TTIP precursors on the perfluorosilanized substrate and the subsequent formation of titanium dioxide. Compared to impinging precursor molecules, these nucleation centers cannot evaporate anymore and result therefore in the formation of undesired clusters. Furthermore, they act as nucleation points of adsorbed precursor molecules, which might diffuse on the treated substrate surface. Generally, we believe that the adsorbed precursor molecules exhibit a high surface mobility due to the low van der Waals interaction between the trimethyl and the trifluoromethyl surface terminating group, which allows them to readily migrate on the surface and nucleate on titanium dioxide. An indication for

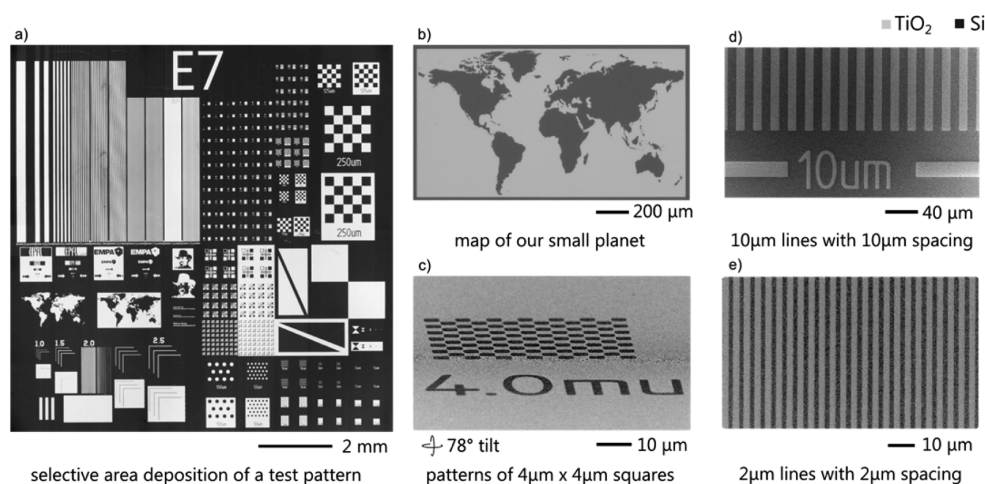


**Figure 7.** Selective area deposition of titanium dioxide (a). Scanning electron micrographs: (b) complex world map geometry, (c) a chess board consisting of rectangles of  $4 \mu\text{m}$  edge length, (d, e) lines of either  $10 \mu\text{m}$  width and  $10 \mu\text{m}$  spacing or  $2 \mu\text{m}$  width and  $2 \mu\text{m}$  spacing.

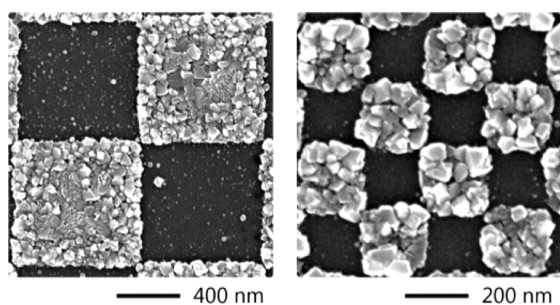


**Figure 8.** High-resolution selective area depositions, obtained by film deposition on passivated surfaces patterned by e-beam lithography and lift-off processes. On the left side, small nucleation sites indicate pinhole defects in the self-assembled monolayer; on the right side we show a high-resolution chess board pattern with rectangles of  $200 \text{ nm}$  side length.

this hypothesis is the higher density of clusters in lower resolution patterns than in higher resolution patterns (compare also Figure 8). In high-resolution patterns the surface diffusion length might be comparable to the critical dimension of the pattern; therefore, the number of visible clusters is reduced. This phenomenon would favor the feasibility of high-resolution patterns. The grain size of the deposited films represents the second problem. It is comparable to the size of the critical dimension of the patterns, which is detrimental to the achieved resolution. While the grain size can be changed by changing growth conditions (e.g., precursor fluxes), this will also influence the maximum selectivity. It has also been reported that doping of titanium dioxide with niobium can be used to form amorphous films;<sup>26</sup> this could improve the obtained resolution. For undoped high-resolution selective area depositions, however, a tradeoff between selectivity (thickness) and grain size must be found.

#### 4. CONCLUSION

We have deposited titanium dioxide selectively utilizing low-temperature HV-CVD and using an established ALD chemistry: titanium isopropoxide and water at an ALD typical growth temperature of  $225 \text{ }^\circ\text{C}$ . The high-vacuum environment allows the simultaneous exposure of the silicon substrate to highly reactive ALD precursor combinations as gas-phase reactions are suppressed.

The selectivity was achieved due to a patterned surface passivation process, where the substrate surface was locally perfluorosilanized using perfluorodecyltrichlorosilane (PFTS) to reduce the interaction between surface and precursor and hence to block film growth. We achieved the patterned silanization by a photo- or e-beam resist-based lift-off process.

We investigated the influence of the silanization layer on the incubation time of the growth and found that the nucleation on the treated substrate surface is significantly delayed compared to the untreated surface. The time difference between the incubation periods represents the selectivity window, in which the selective deposition takes place. Upon longer exposure, selectivity will be lost as nucleation starts to occur also on the treated surface.

Compared to ALD, two additional degrees of freedom are available to optimize the selectivity (the maximum film thickness grown locally): titanium precursor impinging rate and water impinging rate. This is a consequence of the continuous and simultaneous exposure in contrast to ALD. We have shown that the incubation time on both substrate surfaces is dependent on these parameters and optimized the growth conditions to achieve a selective growth of  $(99 \pm 5) \text{ nm}$  for a TTIP impinging rate of  $2.9 \times 10^{14} \text{ molecules cm}^{-2} \text{ s}^{-1}$  and water impinging rates of  $5.7 \times 10^{16} \text{ molecules cm}^{-2} \text{ s}^{-1}$ ; this is a factor of 3 better than previously reported in ALD for the same chemistry. Furthermore, we found that high selectivity is reached in conditions where the precursor deposition efficiency is high and the nucleation delay between treated and untreated surface is used most efficiently.

The highest resolution that we obtained was  $200 \text{ nm}$ . We have, however, encountered that for the maximal selectivity mentioned above, the grain size of the films grown in these conditions are in the same order of magnitude and hence hinder even smaller resolution. The grain sizes can be altered by changing the deposition conditions; however, selectivity will decrease as well in this case. Generally, a trade-off must be found for the realization of high-resolution and high-selectivity depositions.

We believe that low-temperature HV-CVD is a suitable technique for the selective deposition of a broad variety of thin functional films, offering high selectivity and high-resolution capabilities at low substrate temperatures ( $T < 250 \text{ }^\circ\text{C}$ ). The process is optimized in a straightforward fashion by the

alteration of precursor impinging rates and can be transferred to other precursor combinations or materials that have been previously described in ALD literature.

## AUTHOR INFORMATION

### Corresponding Author

\*E-mail: michael.reinke@empa.ch.

### Author Contributions

The manuscript was written through contributions of all authors. All authors have given approval to the final version of the manuscript.

### Funding

The authors gratefully acknowledge the partial financial support of the Swiss National Science Foundation under Contract No. 200021\_13504.

### Notes

The authors declare no competing financial interest.

## ABBREVIATIONS

CMOS, complementary metal–oxide–semiconductor  
CVD, chemical vapor deposition  
HV-CVD, high-vacuum chemical vapor deposition  
ALD, atomic layer deposition  
TTIP, titanium tetraisopropoxide  
PFTS, perfluorodecyltrichlorosilane

## REFERENCES

- (1) Williams, K. R.; Gupta, K.; Wasilik, M. Etch rates for micromachining processing-Part II. *J. Microelectromech. Syst.* **2003**, *12*, 761–778.
- (2) Wolf, S.; Tauber, R. N. *Silicon Processing for the VLSI Era: Process Technology*; Lattice Press: Sunset Beach, CA, 1986.
- (3) Smit, M.; van der Tol, J.; Hill, M. Moore's law in photonics. *Laser Photonics Rev.* **2012**, *6*, 1–13.
- (4) Washburn, A. L.; Bailey, R. C. Photonics-on-a-chip: recent advances in integrated waveguides as enabling detection elements for real-world, lab-on-a-chip biosensing applications. *Analyst* **2011**, *136*, 227–236.
- (5) Crunteanu, A.; Hoffmann, P.; Pollnau, M.; Buchal, C. Comparative study on methods to structure sapphire. *Appl. Surf. Sci.* **2003**, *208–209*, 322–326.
- (6) Tomioka, K.; Tanaka, T.; Hara, S.; Hiruma, K.; Fukui, T. III-V Nanowires on Si Substrate: Selective-Area Growth and Device Applications. *IEEE J. Sel. Top. Quantum Electron.* **2011**, *17*, 1112–1129.
- (7) Jones, S. H.; Lau, K. M. Selective Area Growth of High-Quality GaAs by OMCVD using Native Oxide Masks. *J. Electrochem. Soc.* **1987**, *134*, 3149–3155.
- (8) Allen, S. D. Laser chemical vapor deposition: A technique for selective area deposition. *J. Appl. Phys.* **1981**, *52*, 6501–6505.
- (9) Utke, L.; Hoffmann, P.; Melngailis, J. Gas-assisted focused electron beam and ion beam processing and fabrication. *J. Vac. Sci. Technol., B* **2008**, *26*, 1197–1276.
- (10) Higashi, G. S.; Fleming, C. G. Patterned aluminum growth via excimer laser activated metalorganic chemical vapor deposition. *Appl. Phys. Lett.* **1986**, *48*, 1051–1053.
- (11) Reinke, M.; Kuzminykh, Y.; Hoffmann, P. Limitations of patterning thin films by shadow mask high vacuum chemical vapor deposition. *Thin Solid Films* **2014**, *563*, 56–61.
- (12) Mackus, A. J. M.; Bol, A. A.; Kessels, W. M. M. The use of atomic layer deposition in advanced nanopatterning. *Nanoscale* **2014**, *6*, 10941–10960.
- (13) Jiang, X.; Bent, S. F. Area-Selective ALD with Soft Lithographic Methods: Using Self-Assembled Monolayers to Direct Film Deposition. *J. Phys. Chem. C* **2009**, *113*, 17613–17625.
- (14) Hitosugi, T.; Yamada, N.; Nakao, S.; Hirose, Y.; Hasegawa, T. Properties of TiO<sub>2</sub>-based transparent conducting oxides. *Phys. Status Solidi A* **2010**, *207*, 1529–1537.
- (15) Sinha, A.; Hess, D. W.; Henderson, C. L. Area selective atomic layer deposition of titanium dioxide: Effect of precursor chemistry. *J. Vac. Sci. Technol., B* **2006**, *24*, 2523–2532.
- (16) Sinha, A.; Hess, D. W.; Henderson, C. L. Area-Selective ALD of Titanium Dioxide Using Lithographically Defined Poly(methyl methacrylate) Films. *J. Electrochem. Soc.* **2006**, *153*, G465–G469.
- (17) Park, M. H.; Jang, Y. J.; Sung-Suh, H. M.; Sung, M. M. Selective Atomic Layer Deposition of Titanium Oxide on Patterned Self-Assembled Monolayers Formed by Microcontact Printing. *Langmuir* **2004**, *20*, 2257–2260.
- (18) Färm, E.; Kemell, M.; Ritala, M.; Leskelä, M. Selective-area atomic layer deposition with microcontact printed self-assembled octadecyltrichlorosilane monolayers as mask layers. *Thin Solid Films* **2008**, *517*, 972–975.
- (19) Huang, J.; Lee, M.; Kim, J. Selective atomic layer deposition with electron-beam patterned self-assembled monolayers. *J. Vac. Sci. Technol., A* **2012**, *30*, 1–5.
- (20) Paz, Y. Self-assembled monolayers and titanium dioxide: From surface patterning to potential applications. *Beilstein J. Nanotechnol.* **2011**, *2*, 845–861.
- (21) Reinke, M.; Kuzminykh, Y.; Hoffmann, P. Low Temperature Chemical Vapor Deposition using Atomic Layer Deposition Chemistry. *Chem. Mater.* **2015**, *27*, 1604–1611.
- (22) Devaprakasam, D.; Sampath, S.; Biswas, S. K. Thermal stability of perfluoroalkyl silane self-assembled on a polycrystalline aluminum surface. *Langmuir* **2004**, *20*, 1329–1334.
- (23) Kuzminykh, Y.; Dabirian, A.; Reinke, M.; Hoffmann, P. High vacuum chemical vapour deposition of oxides: A review of technique development and precursor selection. *Surf. Coat. Technol.* **2013**, *230*, 13–21.
- (24) Reinke, M.; Kuzminykh, Y.; Malandrino, G.; Hoffmann, P. Precursor adsorption efficiency of titanium tetra isopropoxide in the presence of a barium  $\beta$ -diketonate precursor. *Surf. Coat. Technol.* **2013**, *230*, 297–304.
- (25) Chen, R.; Kim, H.; McIntyre, P. C.; Bent, S. F. Investigation of Self-Assembled Monolayer Resists for Hafnium Dioxide Atomic Layer Deposition. *Chem. Mater.* **2005**, *17*, 536–544.
- (26) Kyung-Chul, O.; Yoseb, P.; Kwun-Bum, C.; Jin-Seong, P. The effect of Nb doping on the performance and stability of TiOx devices. *J. Phys. D: Appl. Phys.* **2013**, *46*, 295102.